Role of injection pressure on fuel atomization and spray penetration on the Thevetia peruviana and Jatropha curcas biodiesel blends with nanoparticle

Role of injection pressure on fuel atomization and spray penetration on the Thevetia peruviana and Jatropha curcas biodiesel blends with nanoparticle

Xuan Wang[a], Yaoli Zhang[a], C. Karthikeyan[b], P. Boomadevi[c,*], Josef Marouše[kd,e,f], Omaima Nasif[g], Sulaiman Ali Alharbi[h], Changlei Xia[a,i,*]

[a]*Jiangsu Co-Innovation Center of Efficient Processing and Utilization of Forest Resources, International Innovation Center for Forest Chemicals and Materials, College of Materials Science and Engineering, Nanjing Forestry University, Nanjing, Jiangsu 210037, China*

[b]*Department of Mechanical Engineering, Panimalar Engineering College, Chennai, India*

[c]*Department of Aeronautical Engineering, Sathyabama Institute of Science and Technology, Chennai, India*

[d]*Institute of Technology and Business in České Budějovice, Faculty of Technology, Okružní 517/10, České Budějovice 370 01, Czech Republic*

[e]*University of South Bohemia in České Budějovice, Faculty of Agriculture, Studentská 1668, České Budějovice 370 05, Czech Republic*

[f]*Tomas Bata Univesity in Zlín, Faculty of Management and Economics, Mostní 5139, Zlín 760 01, Czech Republic*

[g]*Department of Physiology, College of Medicine and King Khalid University Hospital, King Saud University, Medical City, PO Box-2925, Riyadh 11461, Saudi Arabia*

[h]*Department of Botany and Microbiology, College of Science, King Saud University, PO Box -2455, Riyadh 11451, Saudi Arabia i DeHua TB New Decoration Materials Co., Ltd., Huzhou, Zhejiang 313200, China*

[*]*Corresponding authors: E-mail addresses: boomajeeva@gmail.com (P. Boomadevi), changlei.xia@njfu.edu.cn (C. Xia).*

ABSTRACT

This study investigates the effect of the injection pressure on the spray characteristics and atomization of the fuel. The novelty of the work lies in examining the injection pressure (IP) at four different scenarios such as 180 MPa, 200 MPa, 220 MPa and 240 MPa. A series of test conducted in the single cylinder engine at three different concentrations of B10 (5% Jatropha curcas and 5% Thevetia peruviana-50 ppm of Fe_2O_3), B20 (5% Jatropha curcas and 5% Thevetia peruviana-50 ppm of Fe_2O_3) and B30 (5% Jatropha curcas and 5% Thevetia peruviana-50 ppm of Fe_2O_3). All the samples were tested for performance and emission characteristics. Based on the procured results, the combination of the dual biodiesel blends improvised the production of higher brake power and lowered specific fuel consumption. Adding two blends together reduced the overall viscosity of the Thevetia peruviana (yellow oleander oil) since the viscosity of the jatropha is lower than the yellow oleander oil. As the concentration of the blends is increased there is a marginal drop in the brake thermal efficiency,

however there is an improvement in the brake specific fuel consumptions. In terms of the combustion efficiency, the heat release rates were improvised upon addition of Fe_2O_3. With regard to the emissions, there is no significant change in the NOx. Nevertheless, there is a drastic reduction in the HC and CO formation has been witnessed. Among various blends, B30 at 240 MPa of IP reported lower emissions than B10 and B20. In order to examine the fuel atomization and spray characteristics, numerical modelling was applied. At 240 MPa, the fuel mixing rates were higher compared to the other injection pressure.

Keywords: Dual fuel, nanocatalyst, jatropha curcas Injection pressure, fuel spray characteristics thevetia peruviana

1. Introduction

Fossil fuels account for about 80% of the energy we use on Earth today, according to the International Energy Agency. Fossil fuel consumption is expected to rise in the near future in order to meet the demands of the human race. Unwanted emissions are a problem with fossil fuel use. CO_2 is the primary greenhouse gas emitted by the use of fossil fuels [**1,2**]. It is well-known that CO_2 gas were released when fossil fuels are burned, which is an primary contributor to global warming. Besides, CO_2 concentration has been increased due to industrialization [**3**]. Owing to the increase in global temperature, the polar ice caps are melting, low-lying areas are being flooded, and the ocean levels are increased [**4,5**]. Other pollutants, such as sulphur dioxide, carbon monoxide, and nitrogen oxides, are also a significant threat to mankind, as they can result in serious health consequences such as chronic asthma, impaired lung function, chronic bronchitis, and cardiovascular disease, among other things [**6,7**]. Numerous studies on alternative fuels have been carried out as a result of the growing demand for lower fuel usage as well as fewer exhaust emissions. They also concentrated on improving the combustion efficiency of the engine through the use of conventional fuels.

Nomenclature

v	velocity of the liquid
M_i	Mass fraction of the blends for species G
D	Mass transfer coefficient
ρ	density of the blends
s	spray radii
h_v	Energy equation stated with respect to the heating value
h_{fe}	Fuel thermal enthalpy
$M_{bd,w}$	Mass fraction of the blends
$\dot{m}^x_{bd,w}$	Mass flow rate of the blends
C_p	Specific heat of the fuel

Table 1 Engine specification.

Engine Manufacture	Kirloskar
Engine capacity (cc)	418
Cylinder	Single
Bore length (mm)	86
Stroke length (mm)	72
Injection type	Common rail direct injection
Compression type	Variable
Compression ratio	17.5:1
Maximum speed	3000 rpm
Rated power	7.5 hp
Kerb weight	125 kg
Engine oil	3.5 L

Table 2 Fuel properties of Jatropha oil.

Fuel	Density kg/m^3	Viscosity mm^2/s	Flash point °C	Calorific Value (MJ/K)	Cetane Number
Diesel	820	4.12	58	45.6	57.5
Jatropha oil	931	28.3	190	39.5	54
Thevetia peruviana	920	34	240	40.5	58

Using domestic and renewable resources, biodiesel produces a clean-burning alternative fuel. Fatty acid alkyl esters derived from animal fats, vegetable oils or recycled greases are used to create the fuel [**8,9**]. Biodiesel can be utilized in CI (diesel) engines in its clear form with minimal or no modifications if it is available. Due to the following reasons of simple to use, nontoxic, biodegradable and practically sulphur and aromatics-free, biodiesel is an excellent alternative to existing fossil fuels [**10**]. Particulates, carbon monoxide, hydrocarbons, and toxics from diesel-powered cars can be reduced by using biodiesel as the secondary fuel. The addition of nanoparticles to the biodiesel will increase the liquid's thermal conductivity. In order to enhance combustion efficiency, it is necessary to increase the thermal conductivity of is improved, the ignition temperature is raised, the ignition delay is shortened, and the ignition delay is decreased when nano additives are used. Adding nano-particles to a CI engine will lower emissions as a result of improved combustion. Thus, it is apparent that the addition of nanoparticles to biodiesel will increase the engine' s performance and emissions [**14,15**].

In addition to the nanoparticles, the efficiency of the engine can be adjusted by increasing the injection pressure. Injection pressure plays the vibrant role in deciding the mixture of fuel and air. Optimized fuel and air mixing leads to increased atomization of the fuel [**16**]. Shammer et al., reviewed the consequences of the injection pressure and injection timing on the biodiesel blends. The effective strategies were examined to achieve the higher combustion rates with least environmental problems. Further the retardation methods related to the in-cylinder pressure, heat release rate and combustion durations were analyzed. Higher pressure leads to the better atomization and proper air-fuel mixing ratio [**17-19**]. Kanth et al., analyzed the effects of injection pressure with the hydrogen blends. Adding hydrogen to the diesel increases the efficiency of the engine with least formation of carbon deposition. Advanced injection timing enhanced the BTE owing to lower pressure and ignition delay [**20**]. Jiaqiang et al. explains the operating parameters such as injection pressure and injection timing on the combustion. Optimum injection angle and injection pressure enhances the engine characteristics. When the blends concentration is increased beyond 30%, there is no use of injection pressure. As the engine pressure is increased the injected fuel mass is also increased which resulted in the higher BSFC.

Further, the injection pressure is directly attributed to the atomization [**21,22**]. The novelty of the current study is to observe the effects of injection pressure on the dual fuel blend concept. Despite the typical biodiesel concept, the dual fuel mode techniques are novel and the variation of the injection pressure under the dual mode fuel operations were limited. Hence the series of test conducted in the fuel blends to examine the performance, combustion and emission characteristics of the biodiesel blends at different injection pressure.

2. Materials and methods

In order to examine the role of injection pressure, a series of tests were conducted in the single cylinder engine. In the current study Kir-loskar CRDi engine was utilized to measure the performance, combustion and emission characteristics. **Table 1** shows the specification of the engine. The engine module contains fuel assembly, engine unit sensors, fuel injector unit and electronic control unit. A series of tests were conducted by varying the engine speed and engine loading conditions. All the sensors were connected to calibrate the engine data such as incylinder pressure, exhaust gas temperature, and injection pressure. Piezoelectric kistler pressure sensor was used to measure the cylinder pressure [**23**]. K-type thermocouple sensors were used to measure the exhaust gas temperature and the engine temperatures [**24**]. Throughout the entire run, the temperature was measured and observed. Testo-350 flue gas analyzer was used to measure the emission of NOx, HC, CO and pollutants. Initially, the engine was allowed to run 15-20 min ideally and each test blends were tested. The uncertainty of the equipment' s was determined using the below equation, the liquid [**11–13**]. As a result, the use of nanoparticles improves biodiesel combustion in CI engines and boosts engine performance. It is also possible to promote better combustion in the engine's combustion chamber by using nanoparticles. The biodiesel's radiative mass transfer is improved, the ignition temperature is raised, the ignition delay is shortened, and the ignition delay is decreased when nano additives are used. Adding nano-particles to a CI engine will lower emissions as a result of improved combustion. Thus, it is apparent that the addition of nanoparticles to biodiesel will increase the engine's performance and emissions [**14,15**].

$$\text{Total uncertainties}\,(\%) = \sqrt{[(0.1)2 + (0.1)2 + (1.0)2 + (0.2)2 + (1.0)2 + (0.5)2\,(1.0)2 + (0.8)2 + (0.4)2 + (0.9)2 + (0.45)2]} \quad (1)$$

From the above equation, the total measure of uncertainty was 2.23%, which is in acceptable limit.

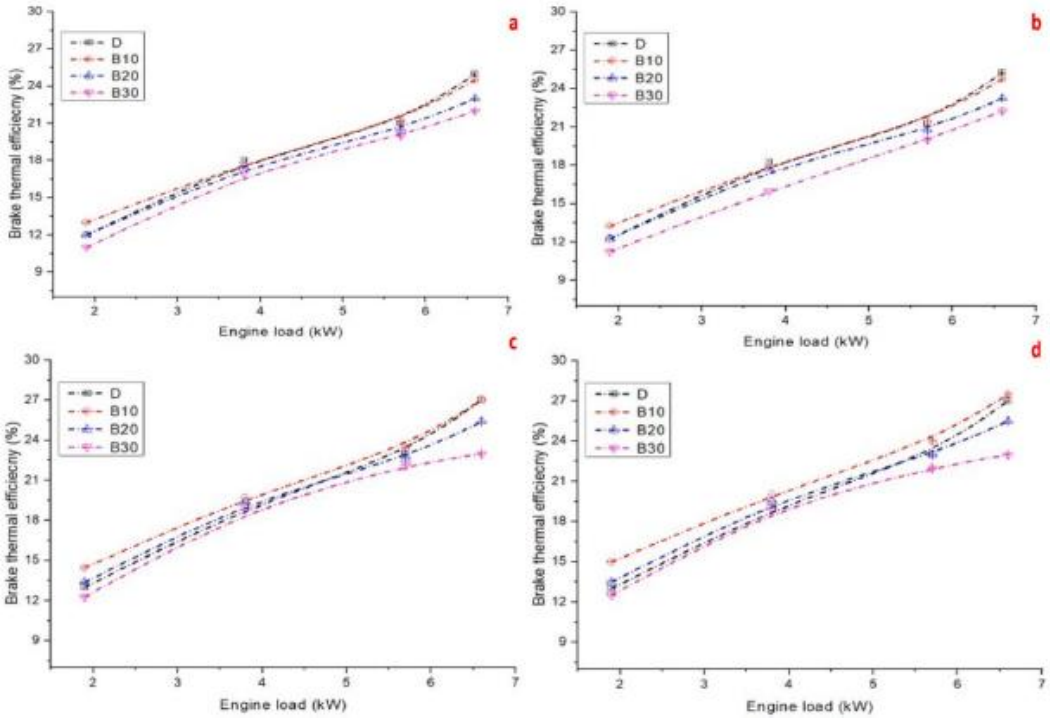

Fig. 1. Variation of brake thermal efficiency a) 180 MPa b) 200 MPa c) 220 MPa d) 240 MPa.

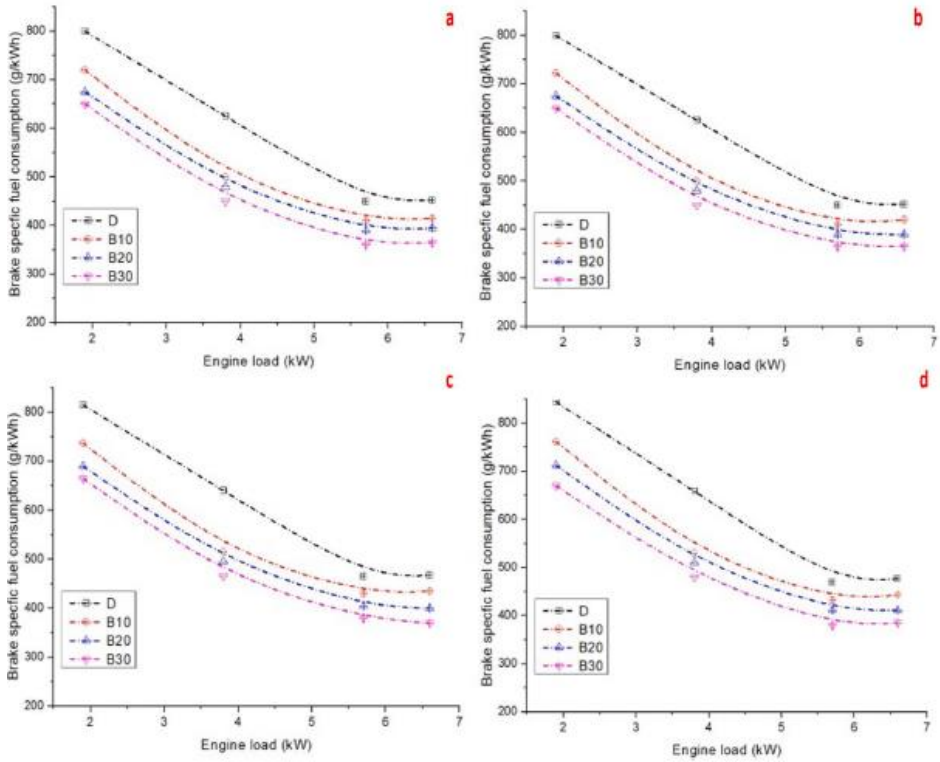

Fig. 2. Variation of brake specific fuel consumption a) 180 MPa b) 200 MPa c) 220 MPa d) 240 MPa.

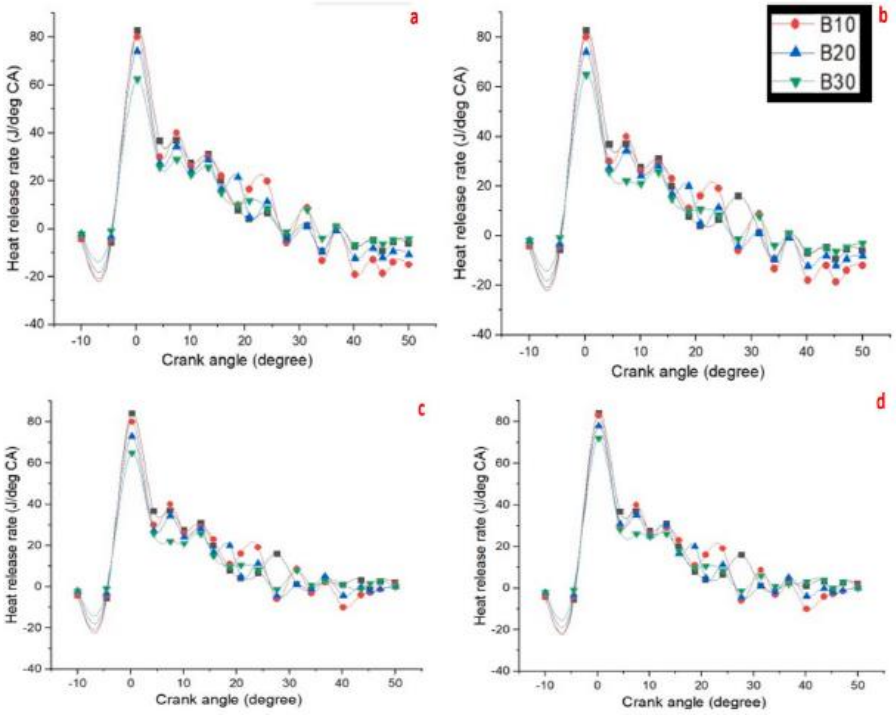

Fig. 3. Variation of Heat release rate a) 180 MPa b) 200 MPa c) 220 MPa d) 240 MPa.

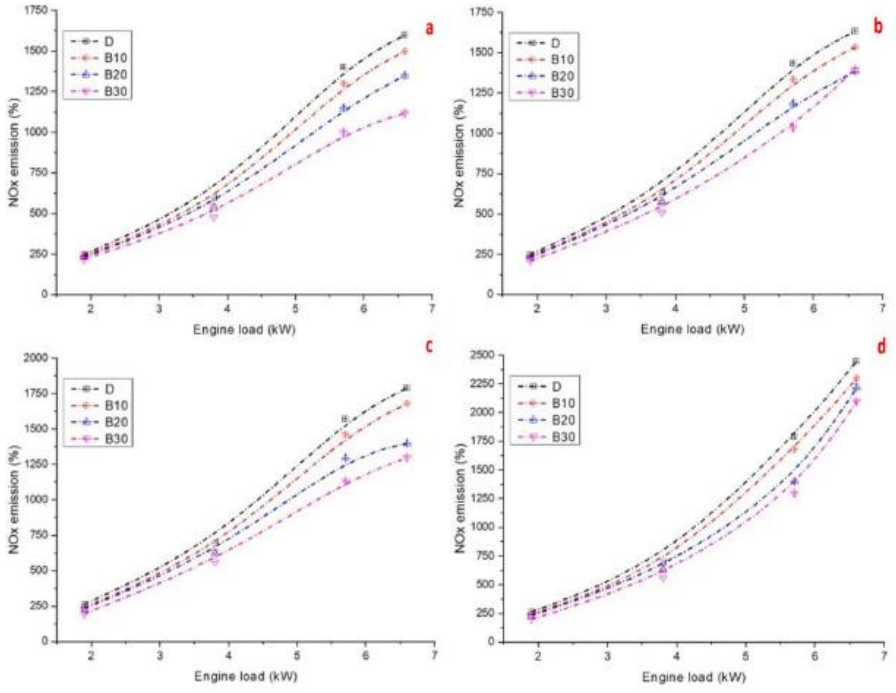

Fig. 4. Variation of NOx emission a) 180 MPa b) 200 MPa c) 220 MPa d) 240 MPa.

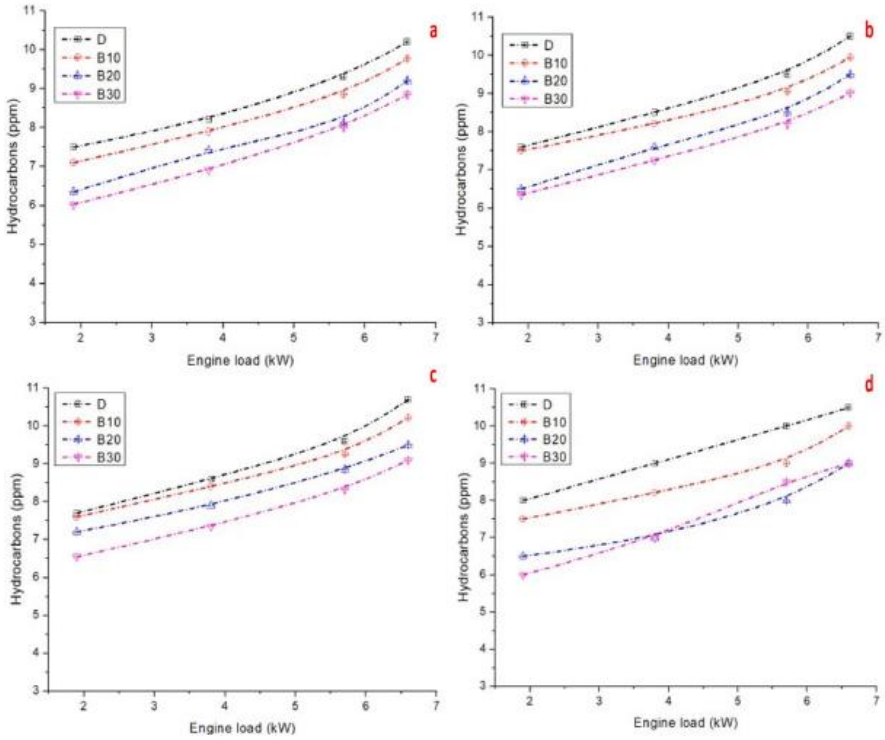

Fig. 5. Variation of Hydrocarbon emission a) 180 MPa b) 200 MPa c) 220 MPa d) 240 MPa.

2.1. Fuel properties

The yellow oleander fruits (Thevetia peruviana) were collected around the urban area. All the collected fruits were dried and deshelled. After removal of all pulps, the kernel was crushed and the oil was extracted [**25,26**]. With regard to the Jatropha curcas, the seeds were collected and dried. After griding the Jatropha seeds, the oil was extracted and filtered for further process. Both Thevetia peruviana and Jatropha curcas oil was undergone transesterification process with the presence of KOH catalyst [**27,28**]. **Table 2** shows the properties of the fuel.

2.2. Numerical simulation

The numerical simulation carried out using the ANSYS-CFX workbench platform. The problem was defined as steady, explicit, and turbulent (shear stress transport). Regarding the meshing, un-structured mesh was used for the domain. In order to examine the spray length different contours were generated and the spray angle and penetration techniques were measured manually based on the pictorial contours [**29,30**].

In order to examine the spray characteristics, the numerical modelling has been introduced based on the Nithya et al.,

$$\rho v \frac{\partial M_i}{\partial s} = \frac{1}{r^2}\frac{\partial}{\partial r}\left(r^2 \rho D \frac{\partial M_i}{\partial r}\right) + G \qquad (1)$$

$$\rho v \frac{\partial M_k}{\partial s} = \frac{1}{s^2} \frac{\partial}{\partial s} \left(s^2 \rho D \frac{\partial M_i}{\partial s} \right) \quad (2)$$

$$\rho v \frac{\partial h_t}{\partial s} - \frac{1}{s^2} \frac{\partial}{\partial s} \left(s^2 \rho D \frac{\partial h_t}{\partial s} \right) = G h_v \quad (3)$$

$$h_{ft} = \int_{Tw}^{T} Cp.dT \quad (4)$$

Eq. (**4**) describes the specific heat of the fuel blends.

$$\rho_w v_w M_{bd,w} - \rho D \left(\frac{\partial M_{bd}}{\partial S} \right)_w = \dot{m}^{x}_{bd,w} \quad (5)$$

Eq. (**5**), signifies the boundary conditions for the model. The model used in the current study was immersed solid [**31-33**]. Two inlets were used to supply both jatropha and oleander oil separately in the volume basis. The part model has been meshed using the multifield reference frame and simulated using shear stress transport turbulence modelling.

3. Results and discussion

In the current study, the series of tests were conducted to observe the effects of dual blends on the diesel engine with regard to the performance (brake thermal efficiency, brake specific fuel consumption), combustion (Heat release rate) and emission characteristics (Nitrogen of oxides (NOx), Carbon dioxide (CO_2), Hydrocarbons (HC), and Smoke opacity). The blends of concentration 10% (5% Jatropha and 5% Thevetia peruviana-50 ppm of Fe2O3), 20% (5% Jatropha and 5% Thevetia peruviana-50 ppm of Fe_2O_3) and 30% (5% Jatropha and 5% Thevetia peruviana-50 ppm of Fe_2O_3) were tested at four different injection pressure of 180 MPa, 200 MPa, 220 MPa and 240 MPa for different engine loading conditions varied from 1.89 kW to 6.6 kW.

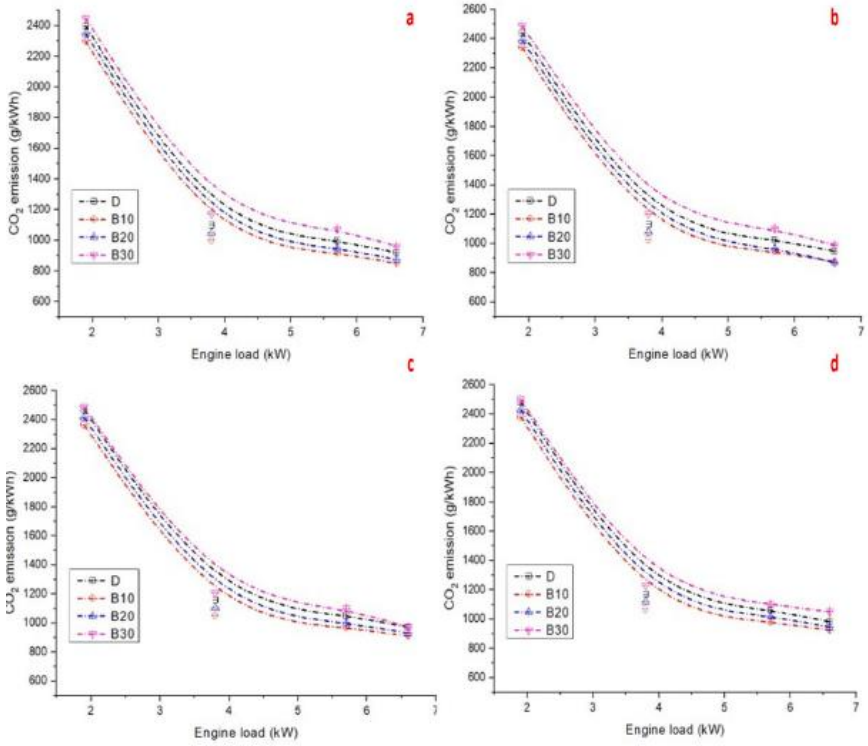

Fig. 6. Variation of CO_2 emission a) 180 MPa b) 200 MPa c) 220 MPa d) 240 MPa.

3.1. Engine performance

Fig. 1 shows the change in the Brake thermal efficiency (BTE) for four different injection pressure. As the engine load increases there is a sharp increase in the production of BTE irrespective of the engine loading. At 1.9 kW of the engine loading, the brake thermal efficiency for B10, B20 and B30 at 180 MPa were 12%, 11.8% and 10.5% and at 200 MPa were 12.3%, 12.2% and 11% and at 220 MPa were 13.7%, 13.5% and 12% and at 240 MPa 13.8%, 13.65% and 13.3% respectively. B20 and B30 reported less BTE compared to neat diesel and B10 despite varying the engine loading at 180 MPa. At the specific injection pressure of 180 MPa, there is no significant change in the BTE between B10 and diesel. The similar behavior has been observed at 200 MPa. B30 reported less BTE than diesel irrespective of changing the injection pressure. Among the various blends, B10 produced the higher BTE than B20 and B30. Addition of the blends at higher concentration to diesel increased the viscosity of the fuel which affects the total burning rate of the fuel. This is the main reason for the drop in the power production. When the injection pressure increases there is a profound change in the BTE [**34,35**]. The blend B20 reported higher brake thermal efficiency than diesel when the injection pressure increased beyond 180 MPa. From the findings it is clear that, increasing the injection pressure is one of the best options to elevate the working thermal efficiency of the any system. Although B20 reported positive results compared to the diesel, when the engine load was maximum there was a shortage in the production of power. When the engine load increase beyond 4.8 kW, there was evidence of drop in BTE for B20. In spite of changing the injection pressure there was also no indication of the improvement in the BTE when the blends concentration was increased beyond 20%.

Fig. 2 represents the change in the brake specific fuel consumption for different brake power. BSFC is one of the important parameters to analyses the efficiency of the engine. In general, the efficiency of the engine is determined based on the consumption of the fuel. Higher fuel consumptions with lower power production leads to high emission of unburnt gases which is a major concern to the

environment. Here, a series of tests were conducted by changing the injection pressure at four different scenarios. From the figure it is evident that, all the blends reported less fuel consumption than diesel. The main reason for the least fuel consumption of B10, B20 and B30 was higher viscosity rates of the blends. As the viscosity of the blends increases the injection rates are affected, only limited fuels enter into the combustion chamber which leads to lower consumption rate and lower BTE indeed [**21,34**]. When comparing the injection pressure to the brake specific fuel consumption, there is no evidence for the significant change in the fuel consumption when the injection pressure is increased. For instance, the blend B30 reported 655 g/kWh, 645 g/kWh, 653 g/kWh and 660 g/kWh at 180 MPa, 200 MPa, 220 MPa and 240 MPa for minimum engine loading condition. Similar to the above, there was no massive change in the consumption rate examined at higher engine load as well. This clearly depicts that the effect of the BSFC on the injection pressure is not significant as expected. However, when the injection pressure is increased the BSFC values were marginally increased irrespective of the engine loading [**35,36**]. Among the blends, B30 reported the lowest BSFC at 6.6 kW loading. The respective BSFC of B30 at 180 MPa, 200 MPa, 220 MPa and 240 MPa were 365 g/kWh, 368 g/kWh, 370 g/kWh and 371 g/kWh. From the findings it is clear that BSFC is increased when the injection pressure is augmented however the change is not monumental.

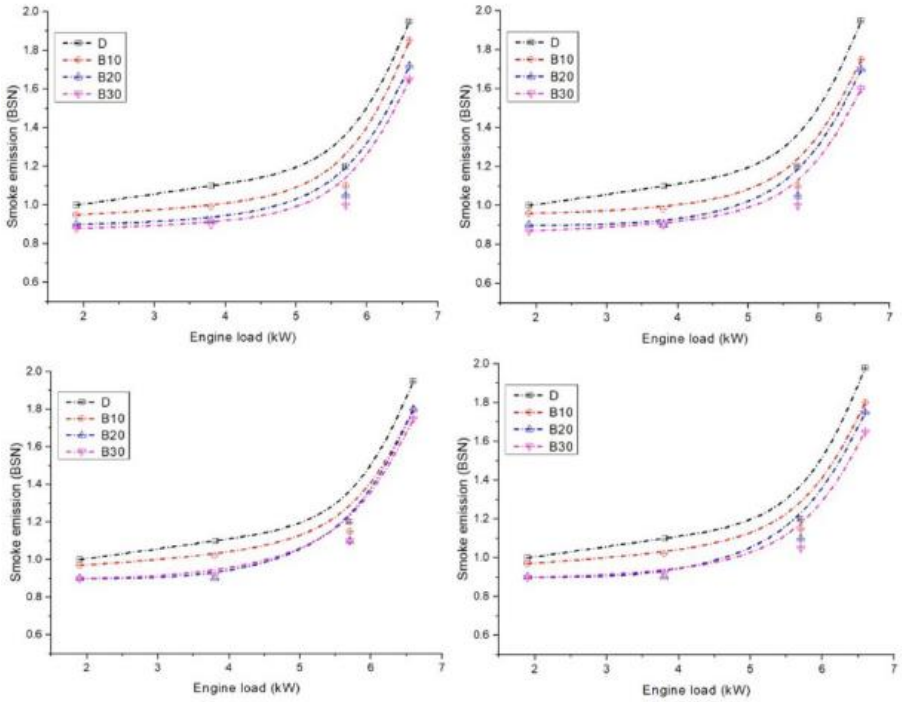

Fig. 7. Variation of smoke emission a) 180 MPa b) 200 MPa c) 220 MPa d) 240 MPa.

3.2. Combustion

Fig. 3 represents the overall heat release rate on the crank angle. Four test samples were analyzed to predict the change in the heat release rate. The maximum HRR was noticed in the diesel compared to the blends. All the blends reported less heat release rate compared to diesel due to the calorific value of the fuel. Since the biodiesel blends have higher viscosity, the heat released during the combustion is low. However, after the crank angle of 5 ° CA, the HRR for the blends are higher due to the diffusion combustion phase. In general, the biodiesel has higher diffusion rates than neat diesel due to the higher oxygen content in the blends [**20,34**]. There is a delay in the initial stage of the combustion

which is the major reason for the drop in the HRR for the biodiesel at the initial crank angles. As the CA degree was increased the HRR for the biodiesel was improved. Moreover, the oscillations in the HRR readings were noted from 10 °CA to 40 °CA. With regard to the injection pressure, there is no evidence for the relation between the HRR to the injection pressure. There is no massive change in the HRR has been noted by varying the injection pressure. For instance, the maximum HRR for the fuel, diesel, B10, B20 and B30 were 83 J/deg CA, 80 J/deg CA, 72 J/deg CA and 60 J/deg CA @ 180 MPa, 81.5 J/deg CA, 79 J/deg CA, 75 J/deg CA and 62 J/deg CA @ 200 MPa, 82 J/deg CA, 80 J/deg CA, 72 J/deg CA and 63 J/deg CA @ 220 MPa, and 80 J/deg CA, 79 J/deg CA, 78 J/deg CA and 75 J/deg CA @ 240 MPa. From the obtained data it is clear that there are no major deviations in the HRR, However, there is a slight change for the blends B20 and B30 at the injection pressure of 220 MPa and 240 MPa.

3.3. Emission characteristics

To examine the quality for the combustion and the emission, the data were drawn and represented in terms of NOx, HC, CO_2, and smoke for the test fuel diesel, B10, B20 and B30 at various injection pressure of 180 MPa, 200 MPa, 220 MPa and 240 MPa respectively.

3.3.1. Nitrogen of oxides emission

Fig. 4 shows the change in the NOx for different engine loading and injection pressure. Typically, the NOx is produced from the unburnt gases after the combustion. Incomplete combustion, inappropriate incylinder pressure and content of the oxygen fuel are the important reasons for the NOx emission. From the findings it is know that, as the engine load is increased there is a slight increase in the production of NOx. Initially the NOx is very low, as the engine load is increased there is high levels of accumulation in the exhaust [**37,38**]. Similarly, as the injection pressure increases there is an increment in the NOx levels. For instance, the maximum NOx production for the B10 blends at 180 MPa, 200 MPa, 220 MPa and 240 MPa were 1480 ppm, 1510 ppm, 1590 ppm and 2255 ppm. The similar trend was noticed for all the blends irrespective of the engine load. Hence it is more evident that increasing the injection pressure leads to higher production of NOx. All blends reported less NOx than diesel owing to lower cylinder temperatures, heating value and latent heat of vaporization. Compared to the diesel, all biodiesel blends operated at lower heating value hence the NOx emissions were low for the blends. Further, injection pressure promotes the fuel and air mixing efficiency. Increasing the pressure creates the strong turbulence in the combustion chamber which leads to pre-mixing and higher NOx rates when the injection pressure is increased from 180 MPa to 240 MPa. Among different blends B30 considered to be producing less NOx at every injection pressure rates of 1000 ppm, 1275 ppm, 1260 ppm, and 2015 ppm respectively. Among the different injection pressures, between 200 and 220 MPa there is no evidence of higher change in the NOx formation.

3.3.2. Hydrocarbon emissions

Hydrocarbons usually formed due to the incomplete combustion of the fuel. The main reason for the incomplete combustion was improper air/fuel mixing ratio and unoptimizable injection pressure. Further, combustion duration and premixed diffusions are also responsible for incomplete combustion. For the efficient combustion, the fuel and air must be atomized and ignited properly [**39,40**]. In addition to the above, adding extra oxygen molecules to the fuel also increases the exergy of the system. Fig. 5 represents the change in the HC for different engine loading conditions for various

injection pressure. All blends reported lower hydrocarbon emissions compared to neat diesel irrespective of engine loading and injection pressure. At 180 MPa, the maximum HC concentrations for diesel, B10, B20 and B30 were 10.1 ppm, 9.1 ppm, 8.7 ppm and 8.2 ppm respectively. As the injection pressure increases there is a slight change in the concentration of hydrocarbons. At 200 MPa, B10 reported higher HC emissions up to 3.9 kW of engine loading compared to 180 MPa. On the other hand, the blends B20 and B30 also reported larger emissions when there is an increase in the injection pressure. When the injection pressure is to be 240 MPa, there is a massive production in the hydrocarbons deposit in the exhaust gases. The maximum HC emissions at 240 MPa were 10.2 ppm, 9.85 ppm, 8.3 ppm, and 8.3 ppm. In 240 MPa, the blends B30 emissions were higher than B20.

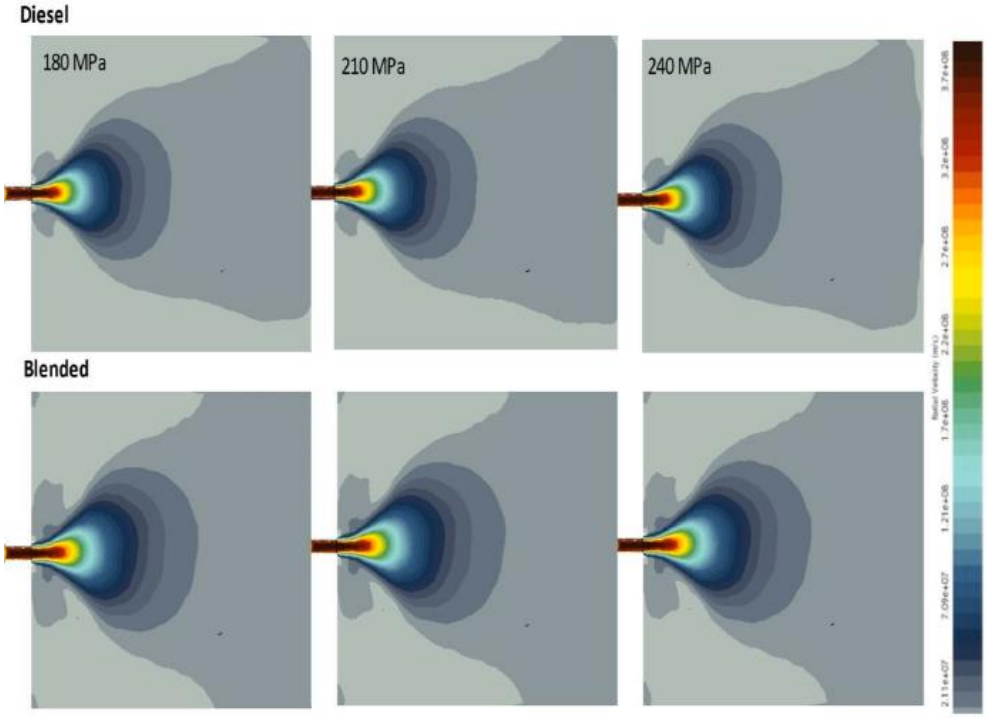

Fig. 8. Variation of smoke emission a) 180 MPa b) 210 MPa d) 240 MPa.

3.3.3. Carbon dioxide emission

According to 2018 data, fossil fuel combustion contributes to 80% of the CO_2 emission. All blends reported lower carbon dioxide emission than diesel due to the reduced number of the carbon atoms present in the test blends. Further, by reducing the viscosity of the blends by pretreatment methods the CO_2 emissions were dropped [**41,42**]. Moreover, the reduction in the emission were not significant owing to the less reaction time and exhaust gas temperature. **Fig. 6** shows the change in carbon dioxide level. As the engine injection pressure increases there is profound increase in the CO_2 emission. At 180 MPa, B30 reported maximum CO_2 emission of 2480 g/kWh which was increased to 2505 g/ kWh when the injection pressure was increased by 20 MPa. Between the 200 MPa to 240 MPa, there is no evidence of increase in the CO_2 emission irrespective of the engine load and test blends. Among different blends, B10 reported least accumulation of CO_2 due to the lower viscosity values compared to B20 and B30. The maximum CO_2 for the blend B30 at 180 MPa, 200 MPa, 220 MPa and 240 MPa were 2480 g/kWh, 2505 g/kWh, 2506 g/kWh and 2506.2 g/kWh.

3.3.4. Smoke emissions

In general, smoke immensely depends on the engine speed and engine loads. **Fig. 7** represents the change in the smoke for various engine loading conditions. The maximum smoke intensity was observed at maximum engine load for all blends. Among blends, B30 produced less smoke compared to other test fuels owing to atomization and vaporization of the blended fuel. Typically, biodiesel produces higher smoke than diesel due the poor fuel atomization [**43,44**]. These effects can be neglected by introduction of the fuel at higher injection pressure. Injecting the fuel at maximum pressure increases the atomization of the blends and reduces the area of the fuel droplets leads to higher fuel-air mixing efficiency indeed. Besides, when the injection pressure is increased, the possibility of the incomplete combustion is also higher. This trends to increase the smoke at high injection pressure [**34**]. From the findings it is clear that the diesel reported the maximum smoke followed by B10, B20 and B30 blends. At 180 MPa, the injection pressure was 1.97 BSN, 1.85 BSN, 1.65 BSN and 1.6 BSN for diesel, B10, B20 and B30 respectively. There is no massive change and smoke is visible by varying the injection pressure. However, the distribution of the smoke at various engine loadings changes related to the injection pressure.

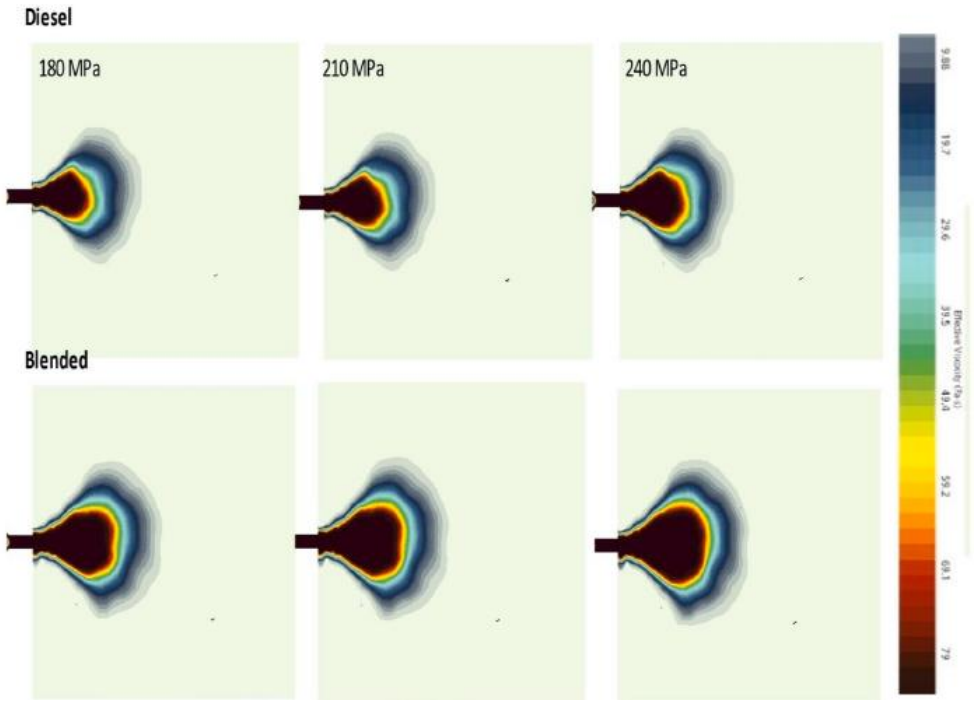

Fig. 9. Variation of smoke emission a) 180 MPa b) 210 MPa d) 240 MPa.

3.4. Numerical simulation

The effects of the injection pressure on the radial velocity, effective viscosity, and relative viscosity of the diesel and B20 blends were determined from the pictorial contours. To examine the change in the spray cone and spray length, the contours were captured at 180 MPa, 200 MPa, 220 MPa and 240 MPa respectively. Fig. 8 shows the change in the radial velocity for the injection pressure 180 MPa, 210 MPa, and 240 MPa. From the procured contours it is clear that the blended fuel reports better distribution compared to the neat diesel. As the injection pressure increases, the spray length has been reduced extremely. However, the formation of the lateral vortices was low at higher injection pressure.

Fig. 9 reports change in the effective viscosity for various injection pressure. From the contour it is clear that diesel fuel reported least spray length compared to the blends which is mainly due to the higher viscosity rates. Further, increasing the injection pressure enhanced the total length of the spray. The same trend was observed in the Fig. 10 as well. From the numerical simulation it is understood that, there is no substantial difference in the diesel and it was observed by varying the injection pressure. This effect is mainly due to the lower viscosity of the diesel compared to biodiesel blends.

4. Conclusion

In the present study, blends were tested at injection pressure of 180 MPa, 200 MPa, 220 MPa and 240 MPa. A series of tests were conducted in the single cylinder engine at three different concentrations of B10 (5% Jatropha and 5% Thevetiaperuviana-50 ppm of Fe_2O_3), B20 (5% Jatropha and 5% Thevetia peruviana-50 ppm of Fe_2O_3) and B30 (5% Jatropha and 5% Thevetia peruviana-50 ppm of Fe_2O_3) to determine the performance, combustion and emission characteristics of the blends. B20 and B30 reported less BTE compared to diesel and B10, despite varying the engine loading at 180 MPa. At the specific injection pressure of 180 MPa, there is no significant change in the BTE between B10 and diesel. On the contrary as the injection pressure is increased to 240 MPa, the B10 reported higher BTE than diesel. On the other hand, B20 also accumulated the BTE levels closer to diesel. Further, the blends reported less fuel consumption than diesel. The main reason for the least fuel consumption of B10, B20 and B30 was higher viscosity rates of the blends. As the viscosity of the blends are increased the injection rates are affected, only limited fuel enters the combustion chamber which leads to lower consumption rate and lower BTE indeed. In terms of the combustion, the blends reported less heat release rate compared to diesel due to the calorific value of the fuel. Since the biodiesel blends has higher viscosity, the heat released during the combustion is low. Nevertheless, there is no evidence of relation between the HRR to the injection pressure. There is no massive change in the HRR varying the injection pressure. With regard to emission, irrespective of the engine load and injection pressure blends reported lowest emission accumulation. However, increasing the injection pressure marginally increases the NOx and HC emissions. Specifically, at higher injection pressure of 240 MPa, there is an increase in the emission compared to 180 MPa and 200 MPa. Meanwhile B10 reported least accumulation of CO_2 due to the lower viscosity values compared to B20 and B30. Based on the numerical study it is predicted that the spray length and the cone angles are different when the injection pressure was elevated to higher levels. Further, the intensity of the spray is higher for the blended fuel at 240 MPa and 220 MPa than 180 MPa. From the series of findings, it is clear that the injection pressure has a potential role in optimizing the engine performance and emission data values. Hence by optimizing the injection pressure there is a huge possibility of enhanced combustion efficiency with least environmental concerns.

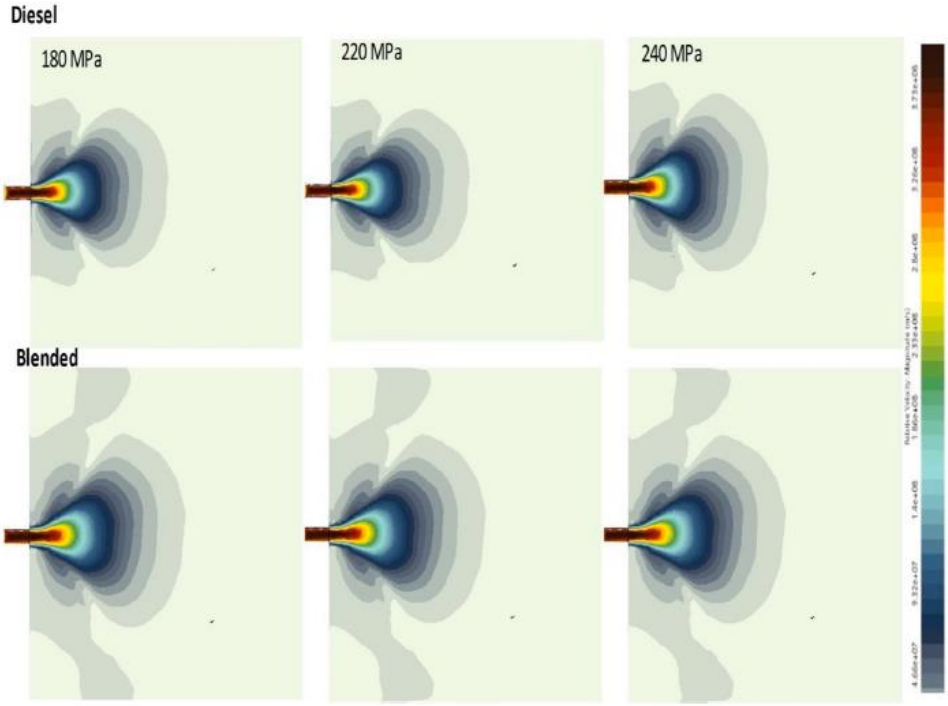

Fig. 10. Variation of smoke emission a) 180 MPa b) 210 MPa d) 240 MPa.

References

[1] Rajak U, Panchal M, Veza I, Agbulut U, Nath Verma T, Saridemir S, et al. Experimental investigation of performance, combustion and emission characteristics of a variable compression ratio engine using low-density plastic pyrolyzed oil and diesel fuel blends. Fuel 2022;319:123720.

[2] Abuhay A, Mengie W, Tesfaye D, Gebino G, Ayele M. Opportunities for New Biorefinery Products from Ethiopian Ginning Industry By-products: Current Status and Prospects. J Bioresour Bioprod 2021;6(3):195-214.

[3] Jandačka J, Mičieta J, Holubčík M, Nosek R. Experimental determination of bed temperatures during wood pellet combustion. Energy Fuels 2017;31(3):2919-26.

[4] Patel A, Shah AR, et al. Integrated lignocellulosic biorefinery: Gateway for production of second generation ethanol and value added products. J Bioresour Bioprod 2021;6(2):108-28.

[5] Ge S, Manigandan S, Mathimani T, Basha S, Xia C, Brindhadevi K, et al. An assessment of agricultural waste cellulosic biofuel for improved combustion and emission characteristics. Sci Total Environ 2022;813:152418.

[6] Sekar M, Ponnusamy VK, Pugazhendhi A, NiZetic S, Praveenkumar TR. Production and utilization of pyrolysis oil from solidplastic wastes: A review on pyrolysis process and influence of reactors design. J Environ Manage 2022;302:114046.

[7] Liu Q, Pachiannan T, Zhong W, Nallusamy N, Zhang Y, Li Z, et al. Effects of injection strategies coupled with gasoline-hydrogenated catalytic biodiesel blends on combustion and emission characteristics in GCI engine under low loads. Fuel 2022;317:123490.

[8] Caqakmak A, Ozcan H. Analysis of combustion and emissions characteristics of a DI diesel engine fuelled with diesel/biodiesel/glycerol tert-butyl ethers mixture by altering compression ratio and injection timing. Fuel 2022;315:123200.

[9] Su M, Li W, Ma Q, Zhu B. Production of jet fuel intermediates from biomass platform compounds via aldol condensation reaction over iron-modified MCM-41 lewis acid zeolite. J Bioresour Bioprod 2020;5(4):256-65.

[10] Judit O, Péter L, Peter B, Monika HR, Jozsef P. The role of biofuels in food commodity prices volatility and land use. J Competitiveness 2017;9(4):81-93.

[11] Teoh YH, Yaqoob H, How HG, Le TD, Nguyen HT. Comparative assessment of performance, emissions and combustion characteristics of tire pyrolysis oil-diesel and biodiesel-diesel blends in a common-rail direct injection engine. Fuel 2022; 313:123058.

[12] Ge S, Brindhadevi K, Xia C, Salah Khalifa A, Elfasakhany A, Unpaprom Y, et al. Enhancement of the combustion, performance and emission characteristics of spirulina microalgae biodiesel blends using nanoparticles. Fuel 2022;308:121822.

[13] Ge S, Brindhadevi K, Xia C, Elesawy BH, Elfasakhany A, Unpaprom Y, et al. Egg shell catalyst and chicken waste biodiesel blends for improved performance, combustion and emission characteristics. Fuel 2021;306:121633.

[14] Hoang AT. Combustion behavior, performance and emission characteristics of diesel engine fuelled with biodiesel containing cerium oxide nanoparticles: A review. Fuel Process Technol 2021;218:106840.

[15] Mujtaba MA, Kalam MA, Masjuki HH, Gul M, Soudagar MEM, Ong HC, et al. Comparative study of nanoparticles and alcoholic fuel additives-biodiesel-diesel blend for performance and emission improvements. Fuel 2020,*279:118434.

[16] Rastogi PM, Sharma A, Kumar N. Effect of CuO nanoparticles concentration on the performance and emission characteristics of the diesel engine running on jojoba (Simmondsia Chinensis) biodiesel. Fuel 2021,286:119358.

[17] Wang RB, Zhou XL, Xu TT, Bian HY, Dai HQ. Research progress on the preparation of lignin-derived carbon dots and graphene quantum dots. J For Eng 2021,6(1): 29-37.

[18] Mehregan M, Moghiman M. Experimental investigation of the distinct effects of nanoparticles addition and urea-SCR after-treatment system on NOx emissions in a blended-biodiesel fueled internal combustion engine. Fuel 2020,262:116609.

[19] Wang R, Wang J, Lai C, Huang C, Lin Z, Yong Q. Enzymatic preparation of glucomannan oligosaccharides and their effects on intestinal microbial proliferation. J For Eng 2021,6(5):96-103.

[20] Kanth S, Ananad T, Debbarma S, Das B. Effect of fuel opening injection pressure and injection timing of hydrogen enriched rice bran biodiesel fuelled in CI engine. Int J Hydrogen Energy 2021,46(56):28789-800.

[21] Jiaqiang E, Pham M, Deng Y, Nguyen T, Duy V, Le D, et al. Effects of injection timing and injection pressure on performance and exhaust emissions of a common rail diesel engine fueled by various concentrations of fish-oil biodiesel blends. Energy 2018,149:979-89.

[22] Saridemir S, Etem Gurel A, Agbulut U, Bakan F. Investigating the role of fuel injection pressure change on performance characteristics of a DI-CI engine fuelled with methyl ester. Fuel 2020,271:117634.

[23] Sangeetha M, Boomadevi P, Khalifa AS, Brindhadevi K, Sekar M. Vibration, acoustic and emission characteristics of the chlorella vulgaris microalgae oil in compression ignition powerplants to mitigate environmental pollution. Chemosphere 2021,30:133475.

[24] Antony Casmir Jayaseelan G, Anderson A, Manigandan S, Elfasakhany A, Dhinakaran V. Effect of engine parameters, combustion and emission characteristics of diesel engine with dual fuel operation. Fuel 2021,302:121152.

[25] Wang Q, Wan FX, Mao P, Luo JY, Zhu K. Composition of essential oil from Cupressus lusitanice and its screened chemical characteristics. J For Eng 2020,5(3): 96-100.

[26] Harari PA, Banapurmath NR, Yaliwal VS, Soudagar MEM, Khan TMY, Mujtaba MA, et al. Experimental investigation on compression ignition engine powered with pentanol and thevetia peruviana methyl ester under reactivity controlled compression ignition mode of operation. Case Studies. Therm Eng 2021,25: 100921.

[27] He Y, Lai P, Xiao Z, Li C, Li J, Zhang A. Study on Ni /HZSM-5 catalytic cracking of Cornus wisoniana oil for bio-hydrocarbon fuel. Renew Sustain Energy Rev 2020,5 (3):66-71.

[28] Tong X, Li Q, Chen W, Zhao L. Alkali extraction of xylan from poplar sawdust and preparation of xylooligosaccharide by enzymatic hydrolysis. J For Eng 2020,5(1): 61-8.

[29] Subramani N, Sangeetha M, Kengaiah V, Prakash S. Numerical modeling on dynamics of droplet in aircraft wing structure at different velocities. Aircraft Eng Aerospace Technol 2022,94(4):553-8.

[30] Ramesh PT, Kengaiah V, Gutema EM, Velusamy P, Balamoorthy D. Development of cost-effectiv e shock tube based on experimental and numerical analysis. Aircraft Eng Aerospace Technol 2022,94(4):559-63.

[31] Battistoni M, Grimaldi CN. Numerical analysis of injector flow and spray characteristics from diesel injectors using fossil and biodiesel fuels. Appl Energy 2012,1(97):656-66.

[32] Zhong W, Mahmoud NM, Wang Q. Numerical study of spray combustion and soot emission of gasoline-biodiesel fuel under gasoline compression ignition-relevant conditions. Fuel 2022,310:122293.

[33] Chen W, Gao R, Sun J, Lei Y, Fan X. Modeling of an isolated liquid hydrogen droplet evaporation and combustion. Cryogenics 2018,96:151-8.

[34] Shrivastava P, Verma TN. Effect of fuel injection pressure on the characteristics of CI engine fuelled with biodiesel from Roselle oil. Fuel 2020,265:117005.

[35] Gad MS, El-Seesy AI, Radwan A, He Z. Enhancing the combustion and emission parameters of a diesel engine fueled by waste cooking oil biodiesel and gasoline additives. Fuel 2020,269:117466.

[36] Raman LA, Deepanraj B, Rajakumar S, Sivasubramanian V. Experimental investigation on performance, combustion and emission analysis of a direct injection diesel engine fuelled with rapeseed oil biodiesel. Fuel 2019,246:69-74.

[37] Serac MR, Aydin S, Yilmaz A, Sevik S. Evaluation of comparative combustion, performance, and emission of soybean-based alternative biodiesel fuel blends in a CI engine. Renew Energy 2020,148:1065-73.

[38] Najafi G. Diesel engine combustion characteristics using nano-particles in biodiesel-diesel blends. Fuel 2018,212:668-78.

[39] Gumus M, Sayin C, Canakci M. The impact of fuel injection pressure on the exhaust emissions of a direct injection diesel engine fueled with biodiesel-diesel fuel blends. Fuel 2012,95:486-94.

[40] Balaji V, Kaliappan S, Madhuvanesan DM, Ezhumalai DS, Boopathi S, Mani S. Combustion analysis of biodiesel-powered propeller engine for least environmental concerns in aviation industry. Aircraft Eng Aerospace Technol 2022,94(5):760-9.

[41] Akcay IH, Gurbuz H, Ak^ay H, Aldemir M. An investigation of euro diesel-hydrogen dual-fuel combustion at different speeds in a small turbojet engine. Aircraft Eng Aerospace Technol 2021,93(4):701-10.

[42] Van Hung T, Alkhamis HH, Alrefaei AF, Sohret Y, Brindhadevi K. Prediction of emission characteristics of a diesel engine using experimental and artificial neural networks. Appl Nanosci 2021. **https://doi.org/10.1007/s13204-021-01781-z**.

[43] Geng L, Bi L, Li Q, Chen H, Xie Y. Experimental study on spray characteristics, combustion stability, and emission performance of a CRDI diesel engine operated with biodiesel-ethanol blends. Energy Rep 2021,7:904-15.

[44] He Y, Lai P, Xiao Z, Li C, Li J, Zhang A. Study on Ni /HZSM-5 catalytic cracking of Cornus wisoniana oil for bio-hydrocarbon fuel. J For Eng 2020,5(3):66-71.